4D-CT Reconstrucion Using Sparsity Level Constrained Compressed Sensing

Haibo Wu, . Wu, A. Maier, H. Hofmann and J. Hornegger are with Pattern Recognition Lab (LME) of Friedrich-Alexander-University Erlangen-Nuremberg. H. Wu and J. Hornegger are also with Graduate School in Advanced Optical Technologies (SAOT) of Friedrich-Alexander-University Erlangen-Nuremberg. R. Fahrig are with Department of Radiology of Stanford University.

***Abstract*—4D-CT is an important tool for treatment simulation and treatment planning in radiotherapy. In order to capture the tumor and tissue movement over time, 4D-CT has to acquire more projection images compared to 3D-CT. This leads to more radiation dose, which is the main concern of the application. Using fewer projections can reduce the radiation dose. However, lack of projections degrades the reconstructed image quality for traditional methods. In this paper, we propose a novel method based on iterative hard thresholding and compressed sensing. We combine the prior knowledge from both methods in our reconstruction problem formulation. In the experiments, we validate our method with XCAT phantom data. The Euclidean norm of the reconstructed images and the ground truth are calculated for evaluation. The results show that our method outperforms the traditional reconstruction method.**

I. Introduction

Four dimensional computed tomography (4D-CT) plays an important role in radiation oncology. Besides the 3D information, 4D-CT also captures the movement of the body's organs over time. With the motion information, the target volume definition is improved and accuracy during treatment delivery for patients with tumors in the abdomen or thorax area is enhanced. [1][2].

In 4D-CT, the projection images are continuously acquired. An additional respiratory signal is recorded at the same time. The projection images are then grouped to different phases according to the amplitude or phase-angle sorting [3-5]. However, to achieve clinically usable image quality, hundreds of projections are needed to reconstruct images of each respiratory phase [6]. Therefore the radiation dose is of great concern for 4D-CT. In order to reduce the radiation dose, the number of projections should be reduced. However, the image quality would be degraded for traditional reconstruction methods. Therefore, prior knowledge is introduced to the reconstruction process. The group of Pan developed the reconstruction method based on compressed sensing [7]. They assume the reconstruction result is smooth and use total variation to promote the smooth solution. Blumensath proposes the iterative hard thresholding method [8]. He uses the sparsity level as the prior knowledge. Both methods can reconstruct the image with much better quality compared to the traditional method ART [9] using only a limited number of projections.

H

In this paper, we propose a 4D-CT reconstruction method based on these two methods. We use the prior knowledge from both methods in our formulation. The details of our method can be found in section 2. The experiments and results are in section 3. Conclusion and outlook in last section.

II. Proposed method

A. Formulation of our method

The 4D object can be described by a sequence of 3D spatial images [10]:

$$\vec{X} = \{\vec{x}_j, 1 \leq j \leq n_t\}, \tag{1}$$

where $\vec{X}$ is the 4D object and $\vec{x}_j$ is the image at j-th respiratory phase. n_t is the total number of reconstructed respiratory phases. Thus, the 4D-CT data acquisition process can be viewed as:

$$\vec{Y} = \{\vec{y}_j = A_j\vec{x}_j, 1 \leq j \leq n_t\}, \tag{2}$$

where $\vec{y}_j$ and A_j are the projection image and system matrix. $\vec{Y}$ stands for projection images. Due to the respiratory motion, we use only the projection images of j-th phase ($\vec{y}_j$) to reconstruct the j-th image ($\vec{x}_j$). Therefore, the reconstruction process can be viewed as solving the linear system:

$$\vec{y}_j = A_j\vec{x}_j + \vec{\gamma}. \tag{3}$$

Here $\vec{\gamma}$ stands for the noise of the measurements. The linear system is ill-posed. There exist infinite solutions. The traditional method formulates the reconstruction problem as:

$$\min_{\vec{x}_j} ||\vec{y}_j - A_j\vec{x}_j||_2. \tag{4}$$

The method finds the solutions which fit the measurements best. Although the minimization problem is convex, there could still be infinite solutions. For example in Fig. 1, the objective function is convex and there is only one global minimum, still the number of minimizers are infinite. To further improve the reconstruction quality, compressed sensing uses sparsity as prior knowledge to choose the best solution in the solution set of (4). It formulates the reconstruction problem as:

$$\min_{\vec{x}_j} ||\Phi\vec{x}_j||_1 \quad s.t. \quad ||\vec{y}_j - A\vec{x}_j||_2 < \lambda. \tag{5}$$

Here, Φ is the sparsifying transform (for example total variation or wavelet transform) and $||\bullet||_1$ stands for L1 norm which calculates the sum of the absolute value of all entries.

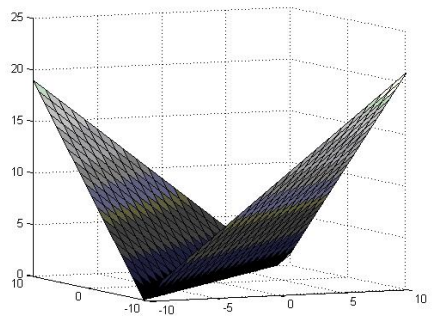

Fig. 1. Example of convex function with non-unique solution

λ describes the energy of the noise. Compressed sensing assumes that medical images can be expressed sparsely by a certain sparsifying transform. For example, most wavelet coefficients of a medical image are zero. Minimizing L1 norm of the coefficients promotes the sparse expression of the image under the corresponding sparsifying transform. Total variation and wavelet are used as sparsifying transforms in compressed sensing based reconstruction methods [7] [11] [12]. Both of them improve the reconstruction quality compared to the traditional reconstruction method, when only limited number of projection images can be used.

Similar as compressed sensing, Blumensath proposes another idea to select the best solution from the solution set of (4). The method is called iterative hard thresholding. The formulation is

$$\min_{\vec{x}_j} ||\vec{y}_j - A\vec{x}_j||_2 \quad s.t. \quad ||\Phi\vec{x}_j||_0 < \alpha, \tag{6}$$

where Φ is again a sparsifying transform and $||\bullet||_0$ is the L0 norm which counts the nonzero entries. For simplicity, we call $||\Phi\vec{x}_j||_0$ sparsity level. α is a scalar describing the actual sparsity level which can be estimated by prior knowledge. In the context of 4D-CT, a prior image can be reconstructed using all projections. Then α can be estimated from this prior image.

The two methods mentioned above use different prior knowledge to improve the reconstruction quality. We propose to combine the prior knowledge in the reconstruction problem formulation. Therefore, we formulate the reconstruction problem as:

$$\min_{\vec{x}_j} ||\Phi_1\vec{x}_j||_1 \quad s.t. \quad ||\vec{y}_j - A\vec{x}_j||_2 < \lambda \quad ||\Phi_2\vec{x}_j||_0 < \alpha. \tag{7}$$

Here, Φ_1 and Φ_2 are two sparsifying transforms. In practice, the noise energy (λ) is not known. The related constraint can be moved to the objective function to make the optimization problem easier. Thus Equation (7) can be rewritten as :

$$\min_{\vec{x}_j} ||\Phi_1\vec{x}_j||_1 + \beta||\vec{y}_j - A_j\vec{x}_j||_2 \quad s.t. \quad |||\Phi_2\vec{x}_j||_0 < \alpha. \tag{8}$$

β is a weighting factor balancing the data fidelity and sparseness. We use total variation as Φ_1 and haar wavelet as Φ_2 in the experiments. Our method promotes a smooth solution which also obeys the sparsity level constraint.

B. Optimization method

It is challenging to solve the optimization problem (8). First of all, as shown in Equation (6), it is a nonconvex optimization problem. Second, in the context of 4D-CT reconstruction, the dimension of the problem is very high. Blumensath proposed a fast and accurate method to solve Equation (6) [8]. The method is proven to converge to a certain local minimum and the accuracy of the solution is guaranteed to be better than the solution of the traditional method. The method deals with the objective function and the constraint separately. It can be summarized:

- Step 1) One gradient descent step to minimize the objective function which is $||\vec{y}_j - A_j\vec{x}_j||_2$ in Equation (6).
- Step 2) Apply the constraint which is $||\Phi\vec{x}_j||_0 < \alpha$ in (6).
- Step 3) Repeat 1 and 2 until the Euclidean norm of two subsquent image estimates is below a threshold.

Blumensath et al. used haar wavelet as Φ. In step 2, they first transform the image estimate to the wavelet domain. Then they keep the α largest wavelet coefficients and set the other wavelet coefficients to zero. Finally they apply the inverse wavelet transform. Similarly, we develop our optimization algorithm as:

- Step 1) One gradient descent step to minimize the objective function which is $||\Phi_1\vec{x}_j||_1 + \beta||\vec{y}_j - A_j\vec{x}_j||_2$ in Equation (8).
- Step 2) Apply the constraint which is $||\Phi_2\vec{x}_j||_0 < \alpha$ in Equation (8).
- Step 3) Repeat 1 and 2 until the Euclidean norm of two subsquent image estimates is below a threshold.

Due to the high dimension, step 1 would be very time consuming if we applied directly one gradient descent step. Pan proposed an efficient method to minimize $||\Phi_1\vec{x}_j||_1 + \beta||\vec{y}_j - A_j\vec{x}_j||_2$ [7]. They split the objective function into two parts which are $||\Phi_1\vec{x}_j||_1$ and $||\vec{y}_j - A_j\vec{x}_j||_2$ and minimize these two parts separately. We use their idea to further speed up the optimization process and our algorithm can be written as:

- Step 1) One step of ART to minimize $||\vec{y}_j - A_j\vec{x}_j||_2$.
- Step 2) Take the result from step 1 as initial, apply k steps of gradient descent to minimize $||\Phi_1\vec{x}_j||_1$.
- Step 3) Apply the constraint which is $||\Phi_2\vec{x}_j||_0 < \alpha$ in Equation (8).
- Step 4) Repeat 1 and 3 until the Euclidean norm of two subsquent image estimates is below a threshold.

III. Experiments and resutls

We used the digital phantom XCAT [13] to validate our method and compare against the state-of-the-art reconstruction method, namely, ART, total variation regularization method (TVR) [7], wavelet regularization method (WR) [11] and iterative hard thresholding method (IHT) [8]. TVR and WR are in fact compressed sensing based reconstruction methods using total variation and wavelets as sparsifying transforms. We generated 360 projection images in fan beam geometry, equally spaced over an entire 360 degree rotation. They

TABLE I
RECONSTRUCTION ERROR OF DIFFERENT METHODS AT ALL PHASES. LOWER VALUES INDICATE A SMALLER ERROR.

	ART	TVR	WR	IHT	Our method
Phase 0	954.129	528.115	491.619	502.797	380.308
Phase 1	955.064	530.937	493.409	504.610	383.991
Phase 2	952.191	519.982	489.499	497.777	380.522
Phase 3	924.856	514.082	464.587	475.610	364.402
Phase 4	909.119	509.091	455.989	468.648	353.299
Phase 5	906.057	507.531	453.293	463.976	348.600
Phase 6	899.210	537.518	448.592	460.021	349.38
Phase 7	891.567	501.844	443.407	454.459	341.703
Phase 8	896.414	496.971	447.953	459.659	347.126
Phase 9	892.580	493.052	435.819	447.010	336.634
Phase 10	903.200	520.333	450.953	461.388	354.010
Phase 11	921.861	518.745	461.159	470.909	354.971
Phase 12	940.355	528.281	473.379	483.011	362.820
Phase 13	944.477	527.099	475.758	487.505	364.099
Phase 14	952.982	527.087	488.380	498.830	376.406
Mean	922.938	517.378	464.920	475.747	359.885

are binned into 15 respiratory phases. Only 24 projeciton images are used for the reconstruction of each phase. The reconstructed image size is 256 x 256 The parameter settings for all methods are chosen to have the best performance. We use 5 gradient descent steps in step 2. Since we do not know the energy of the noise, TVR and WR are formulated as Equation (8) without the sparsity level constraint. The β are set to 0.1 and 0.001 for TVR and WR, respectively.

The reconstruction results of the different methods are shown in Fig. 2. In the first row, there are ground truth, reconstruction results from ART and TVR. In the second row, there are the reconstruction results from WR, IHT and our method, respectively. The result from ART contains severe streak artifacts due to the lack of projections. The streak artifacts are reduced dramatically in the result from TVR but the edges are blurred. The results from WR and IHT keep the edges, but there are still a lot of streak artifacts. Our result is smooth but preserves sharp edges. To quantitatively evaluate the result, we calculate the reconstruction error for each method. The error is calculated as:

$$Error = ||\vec{x} - \vec{x}_{true}||_2 \tag{9}$$

It is in fact the Euclidean norm of the reconstruction result and the ground truth. The evaluation results can be found in Table 1. The smaller number indicates better image quality. TVR, WR and IHT all improve the image quality significantly compared to the traditional method ART. Our method outperforms all the other methods. The reconstruction error of our method is less than 50% of the reconstruction error from ART.

The convergence maps of TVR, IHT, WR and our methods can be found in Fig. 3. The graph shows that our method converges faster than the others and the accuracy of our reconstructed result is the best.

Our method adopts the prior knowledge from TVR and IHT. Therefore, it keeps the advantages of these two methods.

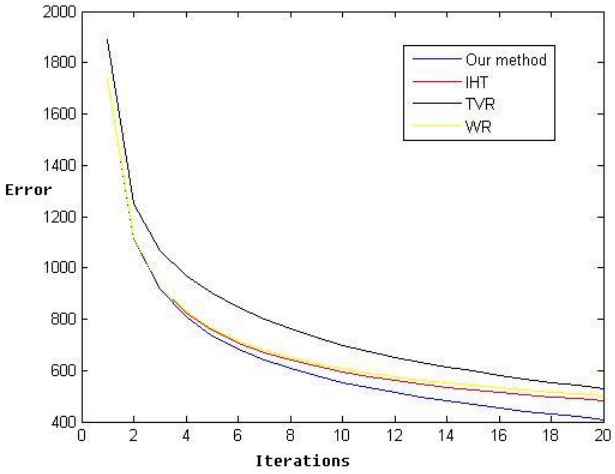

Fig. 3. Convergence maps.

TVR uses total variation as the sparsifying transform and minimizes the total variation of the solution. TVR favors a piecewise constant solution. We also use the total variation in our formulation. Therefore, our method reduces the streak artifacts dramatically and reconstructs a piecewise constant image. IHT uses the sparsity level constraint. IHT assumes that the energy of the real signal should concentrate in the large wavelet coefficients and the energy of noise should concentrate in small wavelet coefficients. Thus, at every iteration step, IHT keeps the α largest wavelet coefficients and sets the others to zero, which keeps the sharp edges and removes the small changes. Our method also uses the sparsity level constraint. Therefore, our method preserves the sharp edges in the reconstruction results.

IV. CONCLUSION AND OUTLOOK

In this paper, we have presented a 4D-CT reconstruction method based on compressed sensing and iterative hard thresholding. The experiments indicate that our method can reconstruct images of improved quality compared to ART when only a small number of projections can be used. However, we only consider prior knowledge in spatial domain in this paper. Using the sparsity in the temporal domain can also improve the reconstructed image quality[14][15]. In the future, we will investigate combining the prior knowledge both in the spatial and temporal domains.

V. ACKNOWLEDGEMENT

The first and last authors gratefully acknowledge funding of the Erlangen Graduate School in Advanced Optical Technologies (SAOT) by the German Research Foundation (DFG) in the framework of the German excellence initiative. The first author thanks the financial support from Chinese Scholarship Council (CSC). The authors thank the financial support from NIH grant R01 HL087917.

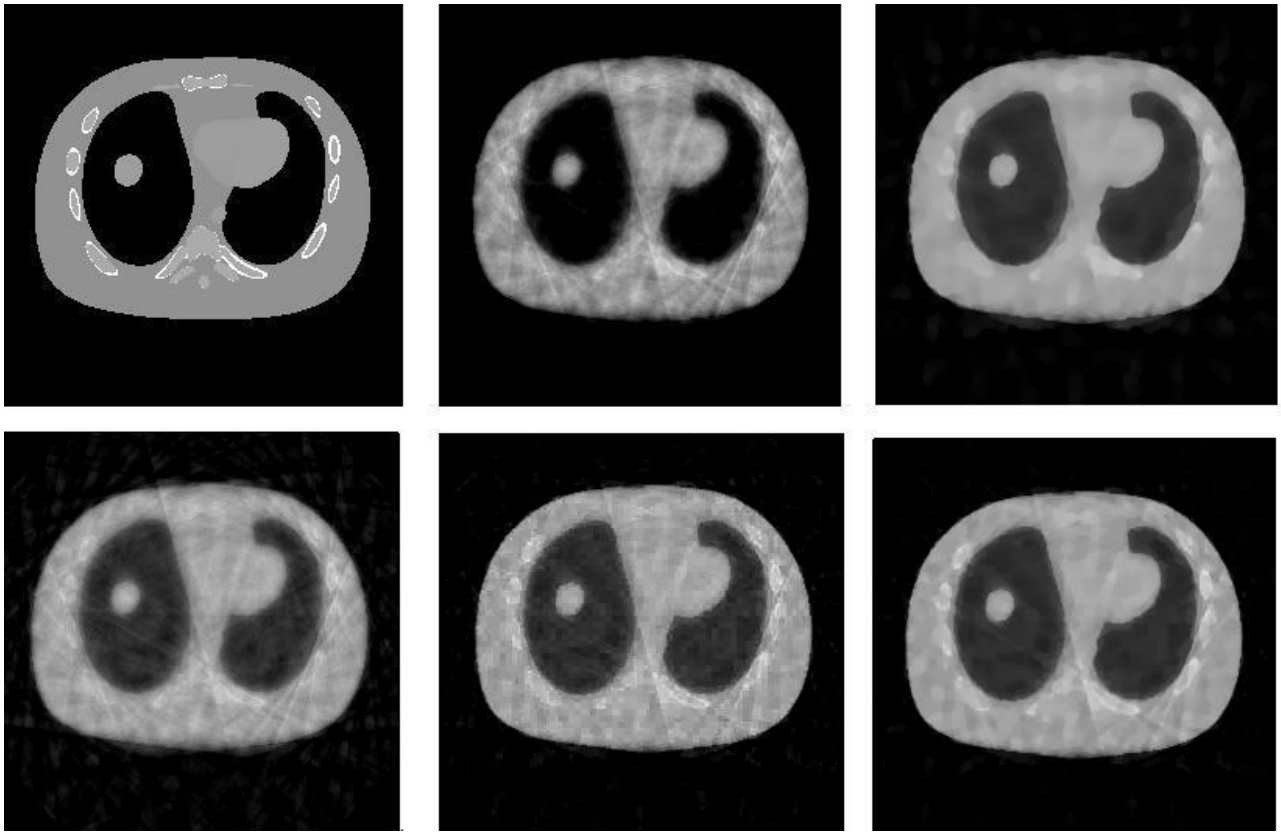

Fig. 2. Reconstruction results of phase 0. All images are set with the same window width and window level. At first row from left to right, they are ground truth, reconstructed images from ART and TVR. At second row from left to right, they are reconstructed images from WR, IHT and our method. The result from ART contains severe streak artifacts due to the lack of projections. The streak artifacts are removed dramatically in the result from TVR but the edges are blurred. The results from WR and IHT keep edges, but there are still a lot of streak artifacts. Our result removes most streak artifacts but keeps sharp edges.

REFERENCES

[1] E. Ford, G. Mageras, E. Yorke and C. Ling, "Respiration-correlated spiral CT: A method of measuring respiratory-induced anatomic motion for radiation treatment planning," *Med. Phys.*, vol. 30, 2003, pp. 88-97.

[2] P. Keall, G. Starkschall, H. Shukla, K. Forster, V. Prtiz, C. Stevens, S. Vedam, R. George, T. Guerrerp and R. Mohan," Acquiring 4D thoracic CT scans using a multislice helical method," *Phys. Med. Biol.*, 2004, vol. 49, 2004, pp. 2053-2067.

[3] D. Low, M. Nystrom, E. Kalinin, P.parikh, J. Dempsey, J. Bradley, S. Mutic, S. Wahab, T. Islam and G. Christensen," A method for reconstruction of four-dimensional synchronized CT scans acquired during free breathing,"*Med. Phys.*, vol. 30, 2004, pp. 1254-1263.

[4] E. Rietzel, T. Pan and G. Chen, "Four-dimensional computed tomography: Image formation and clinical protocol, "*Med. Phys.*, vol. 32, 2004, pp. 333-340.

[5] S.Vedam, P.Keall, V.Kini, H. Mostafavi, H. Shukla and R. Mohan, "Acquiring a four-dimensional computed tomography dataset using an external respiratory signal," *Phys. Med. Biol.*, vol. 48, 2003, pp. 45-62.

[6] D. Ertel, Y. Kyriakou, R. Lapp and W. Kalender," Respiratory phase-correlated micro-CT imaging of free-breathing rodents," *Phys. Med. Biol.*, vol. 54, 2009, pp. 3837-3845.

[7] E. Y. Sidky and X. Pan, "Image Reconstruction in Circular Cone-beam Computed Tomography by Constrained Total-variation Minimization," *Phys. Med. Bio.*, vol. 53, 2008, pp. 4777-4807.

[8] T. Blumensath and M. Davies, "Iterative hard thresholding for compressed sensing," *Applied and Computational Harmonic Analysis*, vol. 27, pp. 265-274, 2009.

[9] G. L. Zeng, Medical Image Reconstruction, *High Education Press*, China, 2009, pp. 145-146.

[10] H. Gao, J. Cai, Z. shen and H. Zhao "Robust principle component analysis based four-dimensional computed tomography," *Phys Med Biol*, vol. 56, 2011, pp. 3181- 3198.

[11] G. Wang and H. Yu, "SART-type image reconstruction from a limited number of projections with the sparsity constraint," *Int. J. Biomedical Imaging 2010*. vol. 2010, 2010, pp. 541-550

[12] H. Wu, C. Rohkohl, and J. Hornegger, "Total variation regularization method for 3-D rotational coronary angiography,"' *Bildverarbeitung fuer die Medizin*, pp. 434-438, 2011.

[13] W. P. Segars, "A realistic spline-based dynamic heart phantom," *IEEE Trans. Nucl. Sci.*, vol. 46, pp.503–506, 2011.

[14] H. Wu, A. Maier, R. Fahrig and J. Hornegger, "Spatial-temporal Total Variation Regularization (STTVR) for 4D-CT Reconstruction," *SPIE*, San Diego, 2012, accepted.

[15] Z. Tian, X. Jia, B. Dong, Y. Lou, and S. B. Jiang, "Low-dose 4dct reconstruction via temporal nonlocal means,," *Med. Phys.*, vol. 38, pp. 1359-1365, 2008.